EFFECT OF SI ADDITION ON THE GLASS FORMING ABILITY AND THERMAL STABILITY OF $Al_{83}Ni_{10}Ce_7$ ALLOY

S.H. Wang, G.M Wang,

Hebei University of Engineering, Handan China, 056038.

Introduction

Al-based amorphous alloys including Al-RE(La, Y, Ce)-TM(Fe, Co, Ni) systems have attracted much attention during the past two decades because of their extraordinary high strength combined with a good ductility [1-5]. It was reported that most Al-based amorphous alloys possess a high tensile strength, as much as 1000 MPa, which is about twice as high as that of conventional high-strength aluminum alloys. The glass-forming ability and the thermal stability of amorphous alloy have attracted greater interest than ever. Inoue has proposed three empirical rulers for the achievement of high glass-forming-ability in metallic glasses: (1) multicomponent alloy systems consisting of more than three elements; (2) significant difference in atomic size ratios above 12% among main three constituent elements; and (3) negative heats of mixing among their elements [6]. The thermal stability of many Al-based glass former has been clearly correlated with chemical composition, for example, generally, by increasing rare earth content or transition metal content from low value.

In the current paper, the effect of Si addition on the glass-forming ability and thermal stability of $Al_{83}Ni_{10}Ce_7$ alloy is closely examined by means of different scanning calorimetry (DSC) and the X-ray diffraction (XRD). The microhardness of $Al_{83}Ni_8Ce_7Si_2$ and $Al_{83}Ni_{10}Ce_7$ has been studied using a Vickers microhardness testing.

Experimental

Ingots of $Al_{83}Ni_8Ce_7Si_2$ and $Al_{83}Ni_{10}Ce_7$ were prepared from the pure elements in an argon atmosphere. Ribbons were produced by a melt-spinning device using a quartz crucible and a copper wheel of 350mm diameter under an argon atmosphere. The amorphous ribbons were ~ 2 mm in width and 30 um in thickness. The amorphous state of the as-quenched ribbons was assessed by XRD (D/max-rB) using Cu K_α radiation. The thermal properties were characterised by using a differential scanning calorimetry (Netzsch DSC404).

Result and discussion

3. Results

To achieve amorphous structure for $Al_{83}Ni_8Ce_7Si_2$ and $Al_{83}Ni_{10}Ce_7$ alloys, ribbon samples were prepared by melt-spinning. Fig. 1 displays the XRD patterns for the melt-spun $Al_{83}Ni_8Ce_7Si_2$ and $Al_{83}Ni_{10}Ce_7$ ribbons at a cooling rate of 36 m/s, revealing the characteristic broad diffraction maxima corresponding to an amorphous phase. Fig. 2 shows the XRD patterns for melt spun $Al_{83}Ni_8Ce_7Si_2$ and $Al_{83}Ni_{10}Ce_7$ ribbons at a cooling rate of 27 m/s. For the $Al_{83}Ni_{10}Ce_7$ ribbon, it is a fully amorphous structure; while for the $Al_{83}Ni_8Ce_5Si_2$ ribbon, it is coexisting amorphous and crystalline phases.

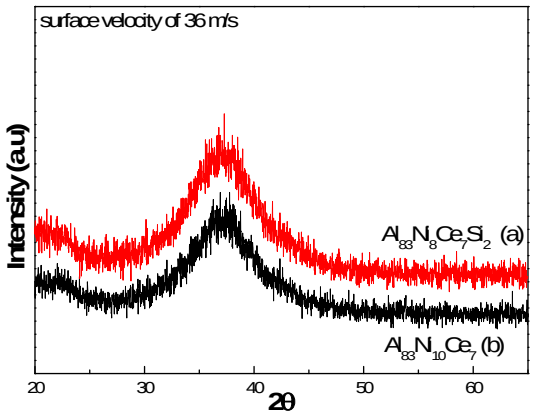

Fig.1. XRD patterns for melt-spun $Al_{83}Ni_8Ce_7Si_2$ (a) and $Al_{83}Ni_{10}Ce_7$ (b) ribbons, showing an amorphous structure at surface velocity of 36 m/s

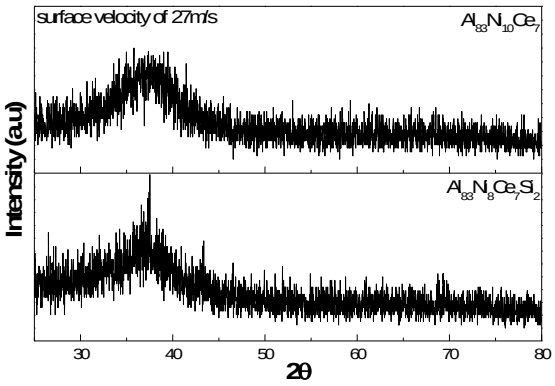

Fig. 2 XRD patterns for melt spun $Al_{83}Ni_8Ce_7Si_2$ and $Al_{83}Ni_{10}Ce_7$ ribbons at a surface velocity of 27 m/s.

The apparent activation energy, E_a, for the crystallization process is usually determined with the Kissinger equation [12]

$$\ln\frac{T^2}{B} = \frac{E_a}{RT} + cons\tan t$$

where B is the heating rate, E_a the activation energy for crystallization, R the gas constant, and T the characteristic temperature such as T_p. By using the

values of T_p and B listed in Table 1, a plot of ln (T^2/B) vs. $1/T_p$ yields approximately straight lines as shown in Fig. 3. According to the slopes of these straight lines, the activation energy is about 305 kJ/mol for T_x, while for the first and second transformation, it is about 388 and 142kJ/mol, respectively.The activation energies for T_x, the first and the second transformation are determined as 487, 426 and 196 kJ/mol, respectively.

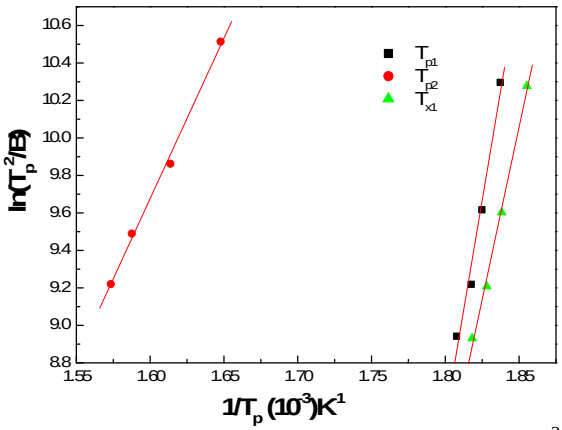

Fig. 3 Kissinger plots between $1/T_p$ and $\ln(T_p^2/B)$ of amorphous $Al_{83}Ni_8Ce_7Si_2$alloy.

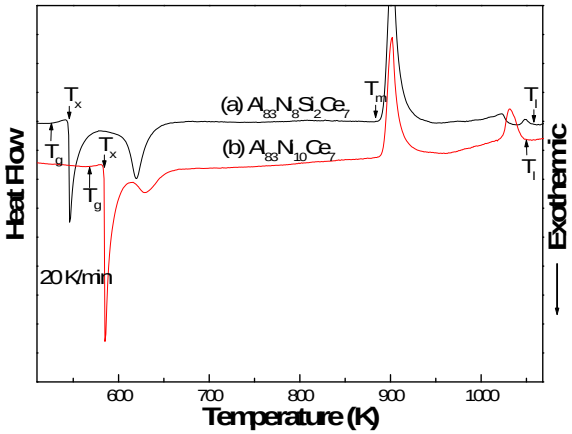

Fig.4DSC curves of as-spun $Al_{83}Ni_8Ce_7Si_2$ (a) and $Al_{83}Ni_{10}Ce_7$ (b) ribbons at a heating rate of 20 K/min.

Fig. 4 shows DSC curves for the amorphous $Al_{83}Ni_8Ce_7Si_2$ and $Al_{83}Ni_{10}Ce_7$ ribbons recorded at a heating rate of 20 K/min. The DSC curves exhibit endothermic reaction corresponding glass transition, followed by the appearance of supercooled liquid region and then crystallization. The T_g, T_x and T_x values are 525, 544 and 18 K, respectively, for $Al_{83}Ni_8Ce_7Si_2$ amorphous alloy; while for the amorphous $Al_{83}Ni_{10}Ce_7$ alloy, those are 566, 584 and 18 K, respectively.

4. Discussion

The activation energy, E_a, for crystallization of an amorphous phase generally arises from two contributions: the activation energy, E_n, for nucleation of crystals and the activation energy, E_g, for subsequent crystal growth. The activation energy for crystallization of the amorphous $Al_{83}Ni_8Ce_7Si_2$ alloy (E_a =305 kJ/mol) is significantly lower than that of the amorphous $Al_{83}Ni_{10}Ce_7$ alloy (E_a =487 kJ/mol), suggesting that the amorphous $Al_{83}Ni_{10}Ce_7$ alloy exhibits a higher thermal stability against crystallization than the amorphous $Al_{83}Ni_8Ce_7Si_2$ alloy.

The activation energy, E_a, for crystallization for the amorphous $Al_{83}Ni_8Ce_7Si_2$ alloy is lower than that of the amorphous $Al_{83}Ni_{10}Ce_7$ alloy. This suggests that different atomic structure exist in the different samples due to the different atomic components. With the replacement of Ni by Si, the Si atoms penetrated in the clearance of Al-Ni-Ce atomic configuration during the solidification. Thus certain atomic rearrangement may become possible. In this case, an amorphous structure consisting of atomic clusters can be obtained. So some atomic clusters may exist in the amorphous matrix for the $Al_{83}Ni_8Ce_7Si_2$ alloy during solidification. The existing atomic clusters will trigger crystalline phase upon reheating, which means that less energy will needed to crystallize upon reheating, in contrast to a more random amorphous structure for the amorphous $Al_{83}Ni_{10}Ce_7$ alloy.

The activation energy, E_a, for the first and second transformation indicated by the DSC is also affected by the replacement of Ni by Si. This may be attributed to the change of the crystalline products with the replacement of Ni by Si. The change of the crystalline product with the replacement of Ni by Si also contributes to change tendency of the heat release of the second transformation of $Al_{83}Ni_8Ce_5Si_2$ and $Al_{83}Ni_{10}Ce_7$ alloy versus heating rate. This needs to be investigated in the further work.

The melt-spun ribbon is seen to maintain good ductility (bending through 180° without fracture) of the amorphous $Al_{83}Ni_8Ce_7Si_2$ and the $Al_{83}Ni_{10}Ce_7$ alloy. The hardness is also tested. A significant decrease in hardenss is observed with the replacement of Ni by Si, suggesting that the random amorphous structure of the $Al_{83}Ni_8Ce_7Si_2$ alloy is different from that of the $Al_{83}Ni_{10}Ce_7$ alloy.

Conclusion

The melt-spun ribbon is seen to maintain good ductility of the amorphous $Al_{83}Ni_8Ce_7Si_2$ and the $Al_{83}Ni_{10}Ce_7$ alloy, while a significant decrease in hardenss is observed with the replacement of Ni by Si.

References

[1] Y. He, S.J. Poon, G.J. ShiØet, Science. 241 (1988) 1640.
[2] Y. He, S.J. Poon, G.J. ShiØet, Scripta Metall. 22 (1988) 1813.
[3] A. Inoue, K. Ohtera, A.P. Tsai, T. Masumoto, Jpn. J. Appl. Phys. 27 (1988) L280, L479, L736.
[4] Y. Kawamura, A. Inoue, T. Masumoto, Scripta Metall. 29 (1993) 25.
[5] R.W. Cahn, Nature. 341 (1989) 183.
[6] A. Inoue, Proc. Jpn. Acad. B. 73 (1997) 19.